

Disruption of sialic acid metabolism drives tumor growth by augmenting CD8⁺ T cell apoptosis

Lenneke A.M. Cornelissen, Athanasios Blanas, Joost C. van der Horst, Laura Kruijssen, Anouk Zaal, Tom O'Toole, Lieke Wiercx, Yvette van Kooyk and Sandra J. van Vliet 

Amsterdam UMC, Vrije Universiteit Amsterdam, Department of Molecular Cell Biology and Immunology, Cancer Center Amsterdam, Amsterdam Infection and Immunity Institute, Amsterdam, The Netherlands

Sialylated glycan structures are known for their immunomodulatory capacities and their contribution to tumor immune evasion. However, the role of aberrant sialylation in colorectal cancer and the consequences of complete tumor desialylation on anti-tumor immunity remain unstudied. Here, we report that CRISPR/Cas9-mediated knock out of the *CMAS* gene, encoding a key enzyme in the sialylation pathway, in the mouse colorectal cancer MC38 cell line completely abrogated cell surface expression of sialic acids (MC38-Sia^{null}) and, unexpectedly, significantly increased *in vivo* tumor growth compared to the control MC38-MOCK cells. This enhanced tumor growth of MC38-Sia^{null} cells could be attributed to decreased CD8⁺ T cell frequencies in the tumor microenvironment only, as immune cell frequencies in tumor-draining lymph nodes remained unaffected. In addition, MC38-Sia^{null} cells were able to induce CD8⁺ T cell apoptosis in an antigen-independent manner. Moreover, low *CMAS* gene expression correlated with reduced recurrence-free survival in a human colorectal cancer cohort, supporting the clinical relevance of our work. Together, these results demonstrate for the first time a detrimental effect of complete tumor desialylation on colorectal cancer tumor growth, which greatly impacts the design of novel cancer therapeutics aimed at altering the tumor glycosylation profile.

Introduction

A major focus of current cancer research is the elucidation of immune evasion strategies employed by malignant cells within the tumor microenvironment (TME). The TME contains a wide variety of cells, including stromal, endothelial and immune cell subsets. The type, density and localization of immune cells within the TME are defined as the Immunoscore, which can be used to predict clinical outcome.^{1,2} As such, cytotoxic CD8⁺ T cells are capable of eliminating tumor

cells and are thus strongly associated with an improved prognosis in many cancer types.³ Nevertheless, as cancers develop, tumor cells acquire the capacity to escape CD8⁺ T cell-mediated cytotoxicity through down-regulation of major histocompatibility complex class I (MHC-I) molecules and expression of immune checkpoint molecules. The transition of immune surveillance to immune escape has been described as the cancer immunoediting hypothesis.⁴ Although cancer immunoediting has been widely studied, the contribution of

Key words: glycosylation, colorectal cancer, sialic acid, CD8⁺ T cell, apoptosis

Abbreviations: CRC: colorectal cancer; MAL-II: *Maaackia amurensis* Lectin II; MC38-MOCK: transfection control MC38 cell line; MC38-Sia^{null}: *CMAS* gene knock out MC38 cell line; MC38-WT: wild type MC38 cell line; Neu5Ac: *N*-acetylneuraminic acid; NK: natural killer cell; NSG: NOD.Cg-Prkdc^{scid} Il2rg^{tm1Wjl}/SzJ; OVA: ovalbumin; Siglecs: Sialic acid-binding immunoglobulin-type lectins; SNA: *Sambucus nigra* agglutinin; ST6Gal1: β -galactoside α 2-6 sialyltransferase 1; TME: tumor microenvironment

Additional Supporting Information may be found in the online version of this article.

Conflict of interest: No potential conflicts of interest were disclosed.

The data that support the findings of our study are available from the corresponding author upon reasonable request.

Grant sponsor: Amsterdam UMC; **Grant number:** PV14-06; **Grant sponsor:** Cancer Center Amsterdam; **Grant number:** CCA2016-5-29;

Grant sponsor: ERC advanced grant; **Grant number:** 339977; **Grant sponsor:** European Union GlyCoCan; **Grant number:** 676421; **Grant**

sponsor: KWF Kankerbestrijding; **Grant number:** VU 2014-6779

DOI: 10.1002/ijc.32084

This is an open access article under the terms of the Creative Commons Attribution-NonCommercial License, which permits use, distribution and reproduction in any medium, provided the original work is properly cited and is not used for commercial purposes.

History: Received 30 Aug 2018; Accepted 10 Dec 2018; Online 22 Dec 2018

Correspondence to: Sandra J. van Vliet, Amsterdam UMC, Vrije Universiteit Amsterdam, Department of Molecular Cell Biology and Immunology, Cancer Center Amsterdam, Amsterdam Infection & Immunity Institute, PO Box 7057, 1007 MB, Amsterdam, The Netherlands, Tel.: +31 20 444 48080; E-mail: s.vanvliet@vumc.nl

What's new?

The current dogma that tumor cells express sialic acids to dampen anti-tumor immunity has led to the development of novel therapeutic strategies aimed at dismantling sialic acid-induced tolerance. Yet the effect of a complete loss of tumor sialylation remains to be elucidated. This study is the first to report a detrimental effect of complete tumor desialylation on colorectal cancer tumor growth, which could be attributed to augmented CD8⁺ T cell apoptosis. The work revisits how tumor-associated sialic acids influence the anti-tumor immune response and has implications for the design of novel cancer therapeutics aimed at altering the tumor glycosylation profile.

cancer-specific glycan structures on immune evasion still remains undefined.

Glycosylation is an enzymatic post-translational process that mediates the attachment of carbohydrate structures to proteins and lipids and functions in a wide range of biological processes including protein folding, cell adhesion and cell signaling.⁵ Compared to their non-malignant counterparts, tumor cells generally harbor an aberrant glycosylation profile of *N*-glycans, *O*-glycans and glycolipids structures that are all known to influence cancer development.^{6,7} The cancer-related glycosylation profile is often characterized by an enhanced expression level of sialylated glycan structures.⁸ Sialic acids (Sias) are a family of nine-carbon monosaccharides with *N*-acetylneuraminic acid (Neu5Ac) as the most common member. Sialylated glycan structures can be recognized by Sialic acid-binding immunoglobulin-type lectins (Siglecs), which are mainly expressed on granulocytes, monocytes, antigen presenting cells and natural killer (NK) cells.⁹ It is generally accepted that Sias are able to skew immune responses toward immune suppression, since most Siglec receptors contain an immunoreceptor tyrosine-based inhibitory motif (ITIM) in their cytoplasmic domain. As Sias, although in lower levels, are also expressed on non-malignant cells, the current dogma states that Sias act as a shield to prevent inappropriate immune reactions against self-antigens. This dampening of immunity by Sias, therefore, led to the concept that glycans represent a self-associated molecular pattern (SAMP) recognized by self-pattern recognition receptors.¹⁰

Indeed, numerous studies have evaluated the negative immunoregulatory function of Sias. Targeting of mouse dendritic cells with Sias conjugated to ovalbumin (OVA) augments the differentiation of regulatory T cells both *in vitro* and *in vivo*.¹¹ Also, Siglec-7 present on NK cells inhibits NK cell cytotoxic activity when stimulated with natural sialylated ligands.^{12,13} Since tumor cells express enhanced levels of Sias, these cells might exploit the sialylation machinery to suppress anti-tumor immune responses. Reduced tumor growth as well as enhanced effector T cell responses and diminished regulatory T cell frequencies were found in a mouse model of B16 melanoma wherein the tumor harbored decreased levels of sialylation.^{14–16} Moreover, a subset of tumor-infiltrating T cells upregulates Siglec-9, which dampens anti-cancer immunity, thus facilitating immune escape by the tumor.¹⁷

The involvement of Sias in suppression of subsequent immune responses, prompted new therapeutic strategies aimed

at reducing tumor-associated Sia expression to enhance anti-tumor immunity. Xiao *et al.* developed an anti-HER2 antibody and sialidase conjugate that simultaneously cleaves Sias from the cell surface and targets tumor cells for antibody-dependent cell-mediated cytotoxicity by NK cells.^{17,18} More recently, intracellular Sia blockade was shown to be sufficient to enhance CD8⁺ T cytotoxicity, resulting in reduced tumor burdens.¹⁶ While these new therapeutic approaches lower the Sia expression of tumors, the effect of complete tumor desialylation on the anti-tumor immune response has never been investigated. Moreover, glycosylation patterns differ substantially between and within tumor types,¹⁹ urging the need to increase our understanding on how tumor-associated glycan structures influence the immune system in tumors of different origins.

With our study we are the first to explore the effect of complete tumor desialylation in colorectal cancer (CRC). The adult gastrointestinal tract is a heavily glycosylated area with distinct regional differences, whereby sialic acid levels are higher in the colon compared to the ileum.^{20–22} Also, recurrence of CRC tumors is correlated with a distinct glycosylation profile, illustrating the relevance of tumor glycosylation in CRC specifically.²³ We assessed tumor growth and the anti-tumor immune response *in vivo* using CRISPR/Cas9 glyco-engineered MC38 CRC cells. Unexpectedly, desialylated MC38 (MC38-Sia^{null}) cells grew significantly faster *in vivo*, which we attribute to decreased CD8⁺ frequencies present within the tumor microenvironment. In addition, we found that MC38-Sia^{null} cells were capable of inducing CD8⁺ T cell apoptosis, likely explaining the reduced CD8⁺ T cells frequencies *in vivo*. Collectively, these results strongly argue that complete tumor desialylation may have detrimental effects on anti-tumor immunity, thus greatly impacting the design of novel cancer therapeutics aimed at targeting the tumor sialylation profile.

Materials and Methods**CRISPR/Cas9 constructs**

CRISPR/Cas9 constructs were made as previously described.²⁴ The following gRNA strands for murine *CMAS* were used: *CMAS* #1: top strand CACCGAATGTGGCCAAACAGTT; bottom strand CTTACACCGGTTTGTCAACAAA; and *CMAS* #2: top strand CACCGTTTCAGAACTTCTTCGA; bottom strand: CAAAGTCTTGAAGAAGCTCAA. The gRNA strands were phosphorylated and annealed prior to cloning in the pSpCas9 (BB)-2A-Puro plasmid, a gift from Feng Zhang (Addgene #62988). Cloning mixtures were treated with PlasmidSafe

exonuclease (Epicentre) to digest residual linearized DNA and used for transformation in XL1-Blue Subcloning-Grade competent bacteria (Stratagene). The Nucleobond Xtra Midi kit (Macherey-Nagel) was used to purify the plasmids. Purified constructs were stored at -20°C until further use.

Generation of the MC38-Sia^{null} cell line

MC38 cells were cultured in DMEM supplemented with 10% heat inactivated fetal calf serum (FCS, Biowest), 1% penicillin and 1% streptomycin. Cells (70–90% confluency) were transfected with CRISPR/Cas9 constructs (3 μg per 6-well) targeting the *CMAS* gene (MC38-Sia^{null}) or an empty CRISPR/Cas9 construct (MC38-MOCK). Lipofectamine LTX with PLUSTM reagent (ThermoFisher Scientific) was used for transfection and applied according to the manufacturer's protocol. After 24 h, fresh medium containing 3 $\mu\text{g}/\text{mL}$ puromycin was added for selection.

Transfected MC38-Sia^{null} cells were incubated with 5 $\mu\text{g}/\text{mL}$ biotinylated Sia-specific *Maackia amurensis* Lectin II (MAL-II, Vector Laboratories) for 1 h on ice, washed with medium and incubated with streptavidin-PE (Jackson ImmunoResearch) on ice. After 1 h cells were washed and sorted in bulk on MAL-II^{low} cells.

To obtain supernatant samples, MC38-MOCK or MC38-Sia^{null} cells were cultured overnight in 96-wells plates at a cell density of 3×10^4 cells/200 μL per well. For heat inactivation, supernatant samples were incubated at 65°C for 5 min.

Surveyor assay

Genomic DNA was isolated with the Quick-DNATM kit (Zymo research) according to the manufacturer's protocol. PCR products (732 bp) for the *CMAS* gene (forward primer: GGCCTGGATTTCAGGAACAT, reverse primer: TGCAGC TGTACCCCAAGCA) were hybridized and treated with Surveyor Nuclease (Surveyor[®] Mutation Detection Kit, Integrated DNA Technologies) and loaded on a DNA agarose gel to visualize presence or absence of the mutation.

Lectin flow cytometry

The biotinylated plant lectins *Sambucus nigra* agglutinin (SNA, Vector Laboratories) and *Maackia amurensis* Lectin II (MAL-II, Vector Laboratories) were used to detect $\alpha 2-6$ and $\alpha 2-3$ Sias, respectively. MC38 cells were incubated with 5 $\mu\text{g}/\text{mL}$ of the lectin for 30 min at 37°C . Cells were washed and incubated with streptavidin-APC (BD Biosciences) for 30 min at 37°C . Cells were washed and acquired on the Beckman Coulter Cyan flow cytometer. Data was analyzed with FlowJo v10.

N-glycan profiling using liquid chromatography mass-spectrometry (LC-MS)

MC38-MOCK and MC38-Sia^{null} cells were washed three times with PBS and resuspended in 100 μL pure water, before homogenization for 45 min in a sonication bath. Samples were

centrifuged (500g, 15 min) and 17.5 μL of pure water was added. Five microliters of reaction buffer (250 mM sodium phosphate buffer; pH 7.5) and 1.25 μL of denaturation buffer (2% SDS in 1 M β -mercaptoethanol) were added. Samples were incubated for 10 min at 100°C to denature the proteins, afterwards 1.25 μL of Triton X-100 and 500 units of PNGase F (QABio, California, USA) were added. Samples were vortexed and incubated overnight at 37°C . The released glycans were then converted to aldoses with 0.1% formic acid, filtered through a protein-binding membrane and dried.

Released N-glycans were fluorescently labeled by reductive amination with procainamide as described previously²⁵ using the LudgerTagTM Procainamide Glycan Labelling Kit (LT-KPROC-24). Procainamide labeled samples were analyzed by HILIC-(U)HPLC-ESI-MS with fluorescence detection. Samples were injected in 24% pure water/76% acetonitrile onto an ACQUITY UPLC[®] BEH-Glycan 1.7 μm , 2.1×150 mm column at 40°C on a Ultimate 3,000 UHPLC instrument (Thermo Scientific, Massachusetts, USA) with a fluorescence detector ($\lambda_{\text{ex}} = 310$ nm, $\lambda_{\text{em}} = 370$ nm). A glucose homopolymer ladder labeled with procainamide (Ludger) was used as a standard. ESI-MS and MS/MS data analysis was performed using Bruker Compass DataAnalysis V4.1 software and GlycoWorkbench software.²⁶

CellTiter-blue[®] cell viability assay

The metabolic activity of MC38 cells was analyzed using the CellTiter-Blue[®] Cell Viability assay (Promega) and measured on the FLUOstar Galaxy (MTX Lab systems, excitation 560 nm, emission 590 nm).

In vivo tumor experiments

C57BL/6, NOD.Cg-Prkdc^{scid} Il2rg^{rm1Wjl}/SzJ (NSG, Charles River) and OT-I mice were used at 8–12 weeks of age and bred at the animal facilities of Amsterdam UMC. For all *in vivo* experiments, an equal distribution of female and male mice was used. Experiments were performed in accordance with national and international guidelines and regulations.

Tumor cells (2×10^5 per mouse) were injected subcutaneously in the flanks. Tumors were measured three times per week in a double-blind manner. Total tumor volume was calculated using the formula $4/3 \times \pi \times abc$ (a = width of the tumor/2, b = length/2 and c = the average of a and b). Mice were sacrificed at day 13 after inoculation or when the tumor reached a size of 2000 mm^3 . Tumor and tumor-draining lymph nodes were isolated and used for further experiments.

Tumor and lymph node dissociation

Tumors were finely minced and enzymatically digested in RPMI containing 1 mg/mL Collagenase type 4 (Worthington), 30 units/mL DNase I type II (Sigma-Aldrich) and 100 $\mu\text{g}/\text{mL}$ hyaluronidase type V (Sigma-Aldrich) for 25 min at 37°C . Lymph nodes were digested with 2 U/mL Liberase TM (Roche) enriched with 30 units/mL DNase I type II for

10 min at 37 °C. All cell suspensions were passed through a 70 µm cell strainer and washed with RPMI supplemented with 10% FCS, 1% penicillin, 1% streptomycin and 1% glutamax. Lymph node digestions were washed twice and directly used for subsequent experiments. Tumor digestion mixtures were loaded on a Ficoll gradient to enrich for lymphocytes and to remove dead cell debris.

Immune cell profiling

Cells were pretreated with 2.4G2 (anti-CD16/32) for 10 min at RT and cell viability was measured using a fixable viability dye (Zombie NIR, Biolegend), 2 µg/mL DAPI or 7-AAD (Invitrogen). Cells were stained for 20 min at RT using the following markers: anti-CD45-PerCp (30-F11), anti-CD31-FITC (390), anti-CD3-BV510 (17A2), anti-CD4-A700 (GK1.5), anti-CD8b-FITC (YTS156.7.7), anti-PD-1-BV785 (29F.1A12), anti-NK1.1-PE/Dazzle 594 (PK136), anti-NKp46-BV421 (29A1.4) (all from Biolegend) and anti-CD8b-APC (eBioH35-17.2, eBioscience). To stain for Foxp3, cells were fixed and permeabilized according to the manufacturer's protocol (Foxp3 Transcription Factor Staining buffer set, eBioscience) and incubated with anti-Foxp3-PE antibodies (150D, Biolegend) for 20 min at RT. For tetramer staining, fluorophore-conjugated MHC-I peptide complexes were added to the cells prior to cell surface staining. The Dpgt1-H-2K^b, Repts1-H-2D^b and Adpgk-H-2D^b tetramers were obtained through the NIH Tetramer Core Facility (Emory University, Atlanta) and labeled with PE, APC and BV421, respectively. Samples were acquired on BD LSRFortessa™ X-20. Data was analyzed with FlowJo v10.

Generation of activated OT-I CD8⁺ T cells

To obtain activated CD8⁺ OT-I T cells, an OT-I spleen was minced and meshed through a 70 µm cell strainer. Cells were cultured in RPMI supplemented with 10% heat inactivated FCS, 1% penicillin, 1% streptomycin, 1% glutamax and 50 µM 2-Mercaptoethanol at a concentration of 3.5×10^6 splenocytes/mL in presence of 0.75 µg/mL OVA₂₅₇₋₂₆₄ peptide. After 3 days, 2 mL medium containing 10 U/mL rmlL-2 was added. At day 5 of culture, CD8⁺ T cells were purified using Lympholyte separation medium (Cedarlane) and checked for purity by staining for CD8b (>90%).

T cell cytotoxicity assay

MC38-MOCK and MC38-Sia^{null} cells were labeled with CFSE (ThermoFisher) and CellVue® Claret (Sigma) respectively, according to the manufacturer's protocol. After labeling, cells were pulsed with the OVA₂₅₇₋₂₆₄ peptide for 2 h at 37 °C. MC38-MOCK and MC38-Sia^{null} cells were plated with or without activated OT-I CD8⁺ T cells and after 5 h of incubation, cells were stained with anti-CD45 and DAPI and acquired on BD LSRFortessa™ X-20. Data was analyzed with FlowJo v10. Tumor cell viability was calculated by dividing the number of viable MC38 cells incubated with CD8⁺ T cells

by the number of viable MC38 cells cultured without CD8⁺ T cells x 100%.

CD8⁺ T cell apoptosis assays

Fresh C57BL/6 splenocytes or activated OT-I CD8⁺ T cells were co-cultured with MC38-MOCK or MC38-Sia^{null} cells or supernatants as indicated. PHA-L (Vector Laboratories) (2 µg/mL) was added to the C57BL/6 splenocytes for activation. Cells were stained with anti-CD8b and 7-AAD and subsequently with Annexin V-FITC (in Annexin V buffer, BD Bioscience). Non-apoptotic CD8⁺ T cells were measured on the BD LSRFortessa™ X-20 and analyzed with FlowJo v10.

Colorectal cancer cohort

Dataset GSE39582 was obtained from the Gene Expression Omnibus (GEO, <https://www.ncbi.nlm.nih.gov/gds>).²⁷ The median of *CMAS* gene expression from 566 CRC patients was ranked from low to high and divided into *CMAS*^{high} (median gene expression >300) and *CMAS*^{low} (<150) groups. Both groups were used to analyze the recurrence-free survival.

Statistical analysis

Statistical significance was tested using GraphPad Prism by performing an unpaired nonparametric t-test. Recurrence free survival was displayed in Kaplan–Meier curves and statistical significance was calculated by Log-rank Mantel-Cox test using GraphPad Prism. (**p* < 0.05, ***p* < 0.01, ****p* < 0.001; ns, not significant).

Results

Lack of cell surface Sia expression after *CMAS* gene knockout

We first analyzed the mouse colorectal cancer cell line (MC38 wild type, MC38-WT) for the presence of sialic acids (Sias). Sias, linked in an α2-6 or α2-3 configuration to the underlying galactose residue, can be visualized using the plant lectins *Sambucus nigra* agglutinin (SNA) and *Maackia amurensis* lectin II (MAL-II), respectively. MC38-WT cells displayed high binding of MAL-II, while SNA binding was negative (Fig. 1a), indicating that MC38-WT cells only expressed α2-3 linked Sias. In order to reduce Sia expression on the tumor cell surface, we previously targeted the *SLC35A1* Sia transporter using shRNA, which resulted in decreased, but still detectable levels of Sia¹⁵ (see Fig. 1b for an overview of the sialylation pathway). However, *SLC35A1* was recently shown to be involved in the O-mannosylation pathway as well.²⁸ Hence, for the present study we mutated the *N*-acetylneuraminyltransferase (*CMAS*) gene, which catalyzes the activation of Neu5Ac to 5'-monophosphate *N*-acetylneuraminic acid (CMP-Neu5Ac), the substrate required for the addition of Sia to the growing glycan chain (Fig. 1b). We designed two different CRISPR/Cas9 guideRNAs, targeting distinct regions in the *CMAS* gene. Independent of the guideRNA used, both *CMAS* knockouts (MC38-Sia^{null}) displayed a complete lack of cell

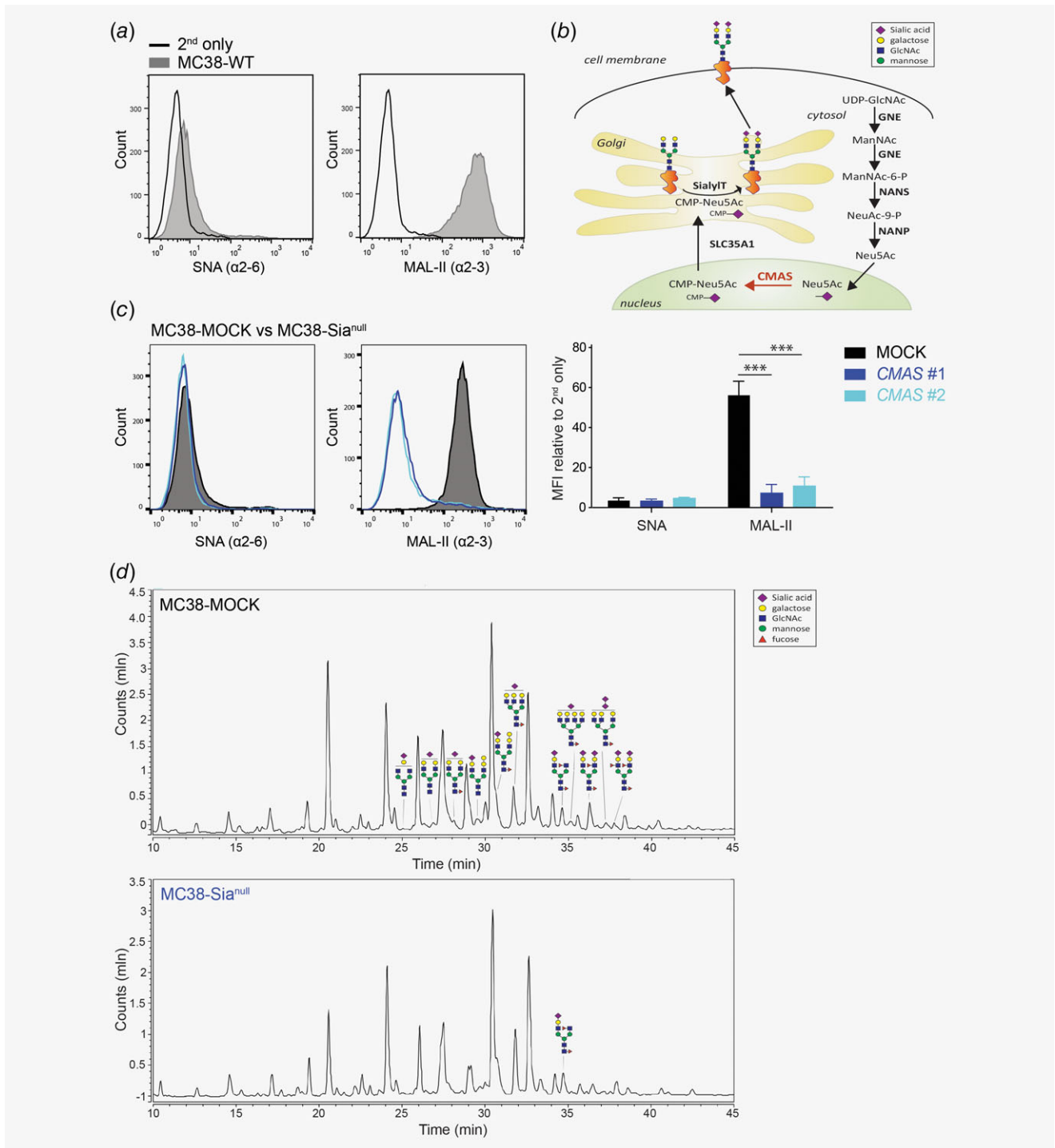


Figure 1. Cell surface sialic acid expression is abrogated in the *CMAS* gene knockout. (a) The presence of α 2-6 and α 2-3 Sia in MC38-WT cells was assessed by flow cytometry using the plant lectins SNA and MAL-II, respectively. (b) Schematic representation of the sialylation pathway. (c) Two CRISPR/Cas9 guideRNAs targeting distinct regions in the *CMAS* gene both completely abrogate MC38 sialylation (MC38-Sia^{null}) as measured with plant lectins SNA and MAL-II. MOCK-transfected MC38 cells (MC38-MOCK) were used as a negative control. Relative mean fluorescence intensities (MFI) were calculated relative to MFI of the 2nd antibody only. Data are representative of three independent experiments (a and c). Mean \pm SD; ***, $p < 0.001$. (d) Liquid Chromatography-Mass spectrometry (LC-MS) analysis of MC38-MOCK (upper) and MC38-Sia^{null} (bottom) sialylation. Only representative examples of the identified sialylated glycans structures are depicted. [Color figure can be viewed at wileyonlinelibrary.com]

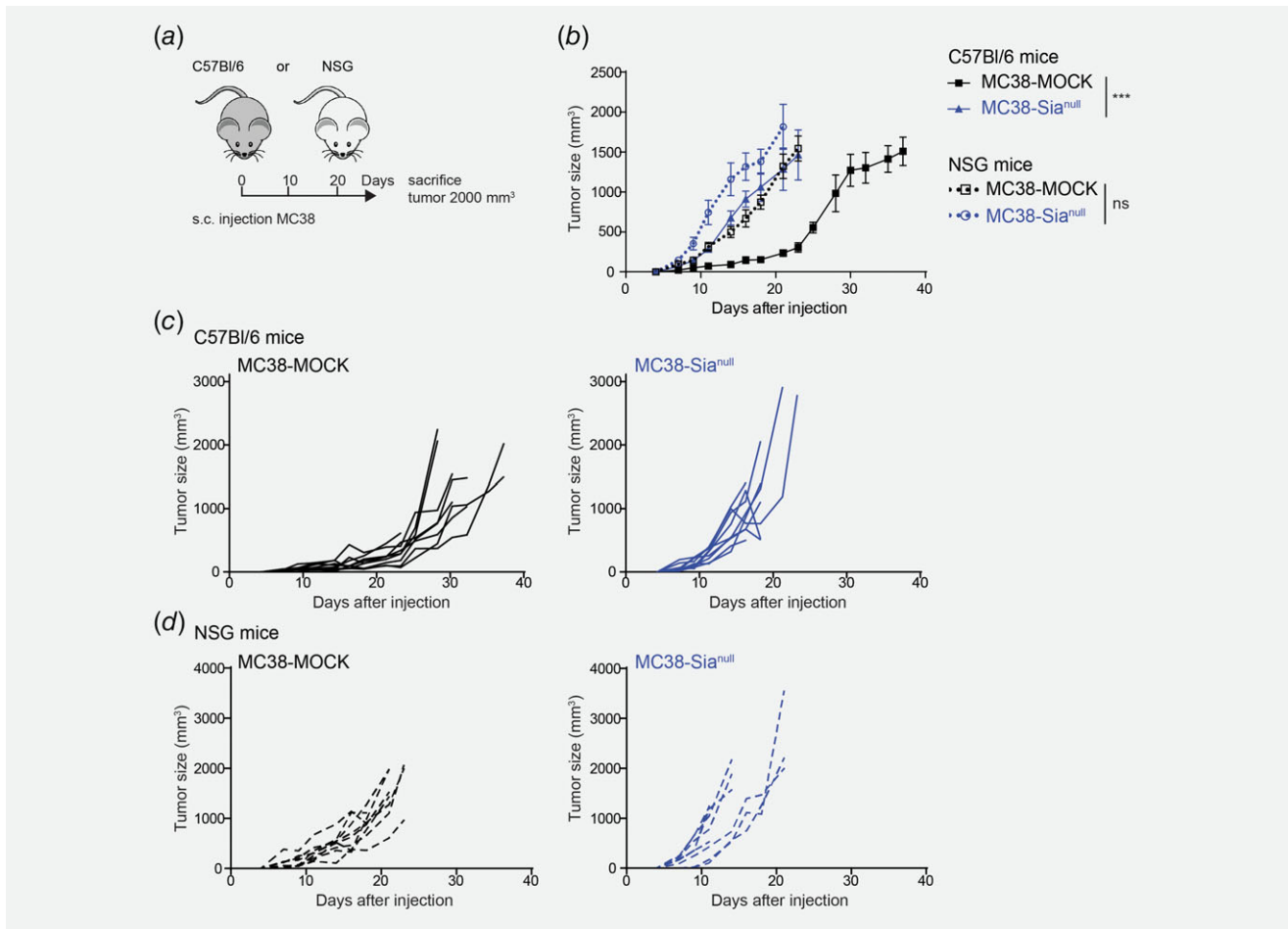


Figure 2. MC38-Sia^{null} tumors display enhanced tumor growth *in vivo*. (a) MC38-MOCK or MC38-Sia^{null} cells were injected into C57Bl/6 mice ($n = 14$) and immunodeficient NOD.Cg-Prkdc^{scid} Il2rg^{rm1Wjl}/SzJ (NSG) mice ($n = 9$). (b–d) Tumor growth was monitored and depicted as mean tumor size (b) or individual tumor growth curves (c and d). Data are representative of one (d) or three (c) independent experiments. Mean \pm SEM; ***, $p < 0.001$; ns, not significant. [Color figure can be viewed at wileyonlinelibrary.com]

surface Sia (Fig. 1c). The *CMAS* gene mutation was confirmed using the Surveyor assay (Supporting Information Fig. 1A) and by mass spectrometric analysis (Fig. 1d and Supporting Information Table S1). We could only detect one minor sialylated glycan structure on MC38-Sia^{null} cells, which we assume is a contamination from the MC38 culture medium.

Manipulation of the glycosylation machinery may influence the proliferation capacity of cells. Nevertheless, MC38-MOCK and MC38-Sia^{null} cells displayed identical growth rates under *in vitro* culture conditions as observed by manual counting and by measuring their metabolic activity (Supporting Information Fig. 1B and C). Thus, we obtained a completely desialylated non-clonal MC38 cell line through CRISPR/Cas9 genome engineering of the *CMAS* gene.

MC38-Sia^{null} cells display enhanced tumor growth *in vivo*

Next, we investigated the effect of complete tumor desialylation on *in vivo* tumor growth by injecting MC38-MOCK and MC38-Sia^{null} cells into C57Bl/6 mice (Fig. 2a). Unexpectedly,

the MC38-Sia^{null} tumors grew significantly faster than MC38-MOCK tumors (Figs. 2b and 2c). The tumor mass, weighed directly after isolation, correlated to tumor size (Supporting Information Fig. 2A), confirming the tumor measurements were accurately performed. Moreover, the MC38-Sia^{null} cells retained their Sia negative phenotype after *in vivo* passage (Supporting Information Fig. 2B).

To ascertain that the differences observed in tumor growth were due to alterations in anti-tumor immunity, we inoculated the MC38-MOCK and MC38-Sia^{null} cells into immunodeficient mice (NOD.Cg-Prkdc^{scid} Il2rg^{rm1Wjl}/SzJ, NSG mice). Compared to immunocompetent mice, MC38-MOCK tumors grew faster in immunodeficient mice, providing evidence for the existence of immune surveillance toward the MC38-MOCK tumors (Figs. 2b and 2d). In contrast, the MC38-Sia^{null} only displayed a small increase in tumor growth in the immunodeficient mice compared to the immunocompetent mice (Figs. 2b and 2d), suggesting in the case of MC38-Sia^{null}, the immune system is less able to recognize or can less efficiently combat

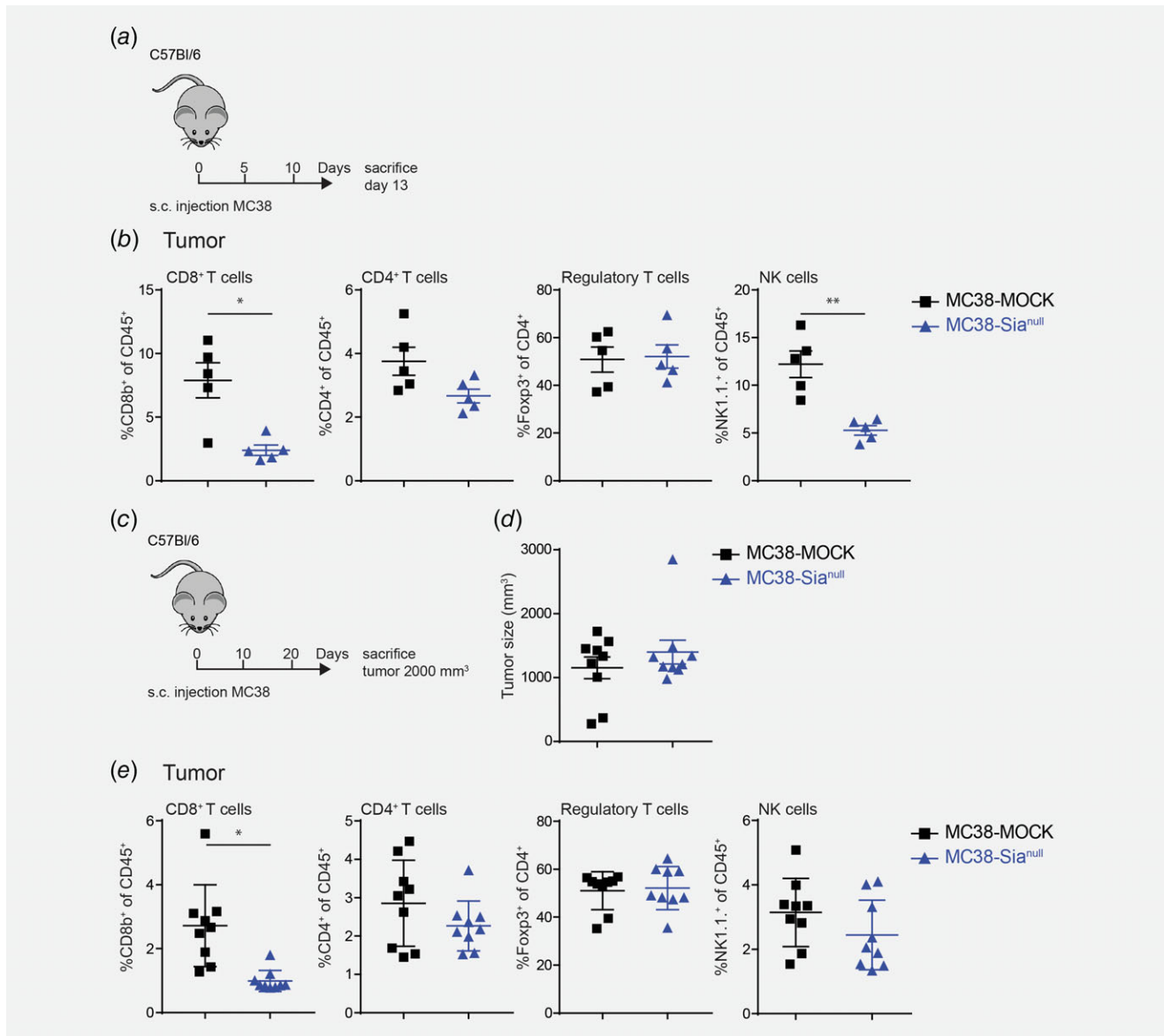


Figure 3. MC38-Sia^{null} tumors harbor less CD8⁺ T cells. MC38-MOCK or MC38-Sia^{null} cells were injected in C57Bl/6 mice and sacrificed at day 13 of tumor development (a, b, n = 5) or when the tumor reached a size of 2000 mm³ (c–e, n = 9). (b) and (e) Flow cytometric analysis of viable, CD45⁺ CD8⁺ T cells (CD3⁺CD8⁺), CD4⁺ T cells (CD3⁺CD4⁺), Regulatory T cells (CD3⁺CD4⁺Foxp3⁺) and NK cells (CD3[−]NK1.1⁺) at tumor site after 13 days of tumor development (b) or when the tumor reached a size of 2000 mm³ (e). Data are representative of two independent experiments (a–e). Mean ± SEM; *, *p* < 0.05; **, *p* < 0.01. [Color figure can be viewed at wileyonlinelibrary.com]

MC38-Sia^{null} tumor outgrowth. Together, our data imply that complete CRC desialylation actually augments tumor growth, which might be attributed to a lack of activation or a heightened suppression of anti-tumor immunity.

MC38-Sia^{null} tumors harbor less CD8⁺ T cells

To explore whether tumor desialylation influences anti-tumor immunity, we analyzed the immune cell composition of the tumor and tumor-draining lymph nodes at day 13 of tumor development (Fig. 3a). Compared to MC38-MOCK, the MC38-Sia^{null} tumors harbored less cytotoxic CD8⁺ T cells and

NK cells, while CD4⁺ T cells tended to be lower in MC38-Sia^{null} tumors (Fig. 3b). Strikingly, frequencies of Foxp3⁺CD4⁺ regulatory T cells were equal in MC38-MOCK and MC38-Sia^{null} tumors (Fig. 3b). Moreover, the reduced levels of CD8⁺ T cells and NK cells were only observed locally at the tumor site, as the tumor-draining lymph nodes contained equal frequencies of all subsets investigated (Supporting Information Fig. 3A).

As MC38 tumors develop, CD8⁺ T cell frequencies seem to drop.²⁹ Thus, the decreased CD8⁺ T cell infiltration in MC38-Sia^{null} tumors might be explained by tumor size, which

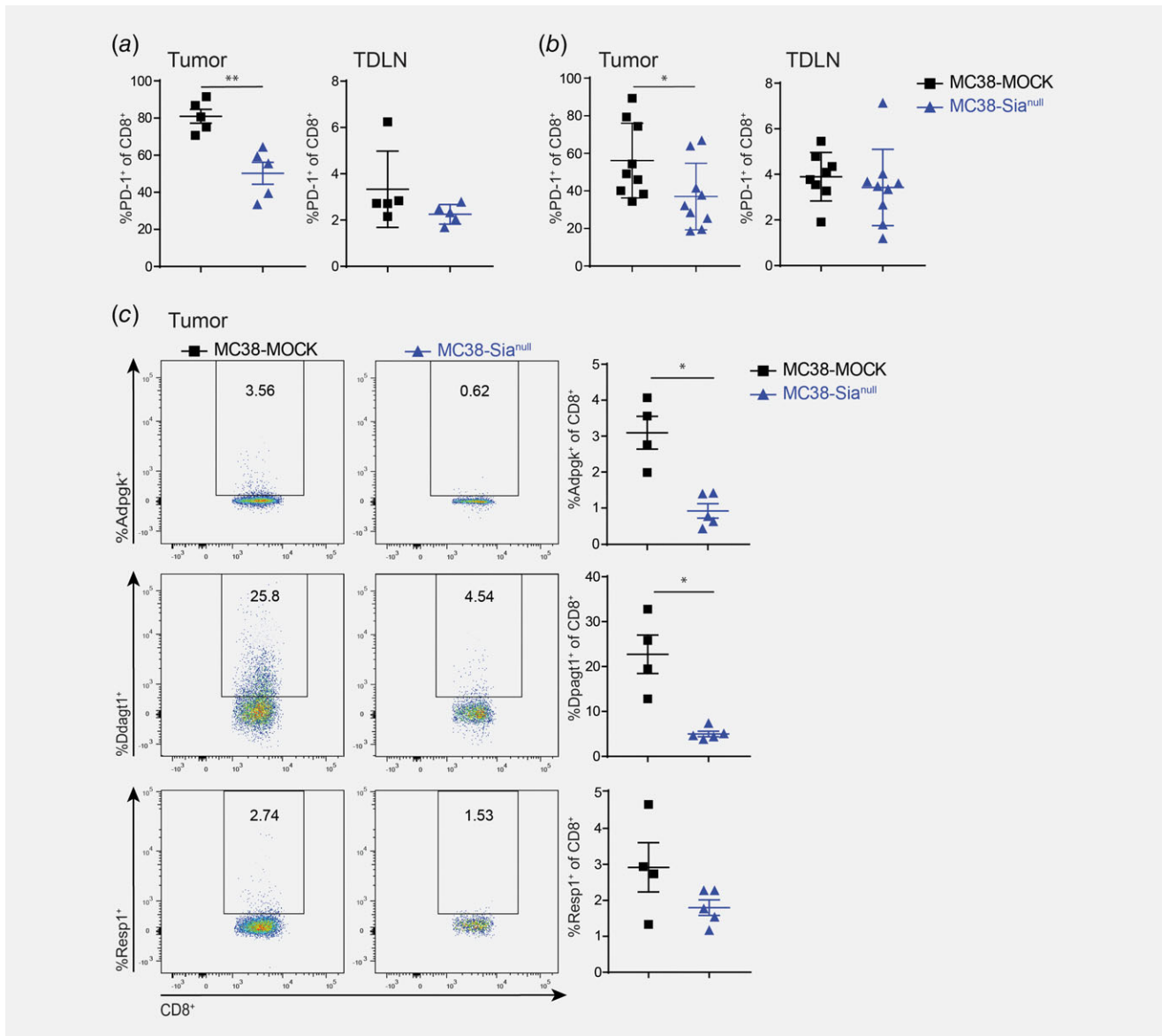


Figure 4. Less PD-1 positive and MC38 neoantigen-specific CD8⁺ T cells at the MC38-Sia^{null} tumor site. (a) and (b) Percentage of PD-1⁺CD8⁺ T cells was analyzed at the tumor location or in tumor-draining lymph nodes with flow cytometry at an early stage of tumor development (a) or when the tumors reached an equal size (b). (c) Tumor infiltrated CD8⁺ T cells (viable CD45⁺CD3⁺CD8b⁺) were stained with tetramers specific for three different MC38 neoantigens²⁹ and analyzed by flow cytometry. Data are representative of two independent experiments. Mean \pm SEM; *, $p < 0.05$; **, $p < 0.01$. [Color figure can be viewed at wileyonlinelibrary.com]

at day 13 is significantly larger for MC38-Sia^{null}, and not by the desialylated phenotype (Supporting Information Fig. 4A). Therefore, we also checked the immune composition when tumors had an identical size of 2000 mm³ (Figs. 3c and 3d). Interestingly, the reduced CD8⁺ T cell frequencies in the MC38-Sia^{null} were maintained in equally sized tumors (Fig. 3e). In contrast to day 13 of tumor development, tumor-infiltrated NK cell frequencies were similar in both MC38-MOCK and MC38-Sia^{null} tumors (Fig. 3e). Again, the levels of Foxp3⁺CD4⁺ regulatory T cells in the tumor (Fig. 3e) and the levels of CD8⁺,

CD4⁺, regulatory T and NK cells in the tumor-draining lymph nodes remained unaffected (Supporting Information Fig. 3B).

Remarkably, also lower frequencies of PD-1⁺CD8⁺ T cells were found in the MC38-Sia^{null} tumors compared to the MC38-MOCK tumors, both at day 13 of tumor development (Fig. 4a) as well as when the tumors had an equal size (Fig. 4b). This effect was solely observed at the tumor site and not in the tumor draining lymph nodes (Figs. 4a and 4b). PD-1 is well-known for its crucial role as a checkpoint molecule in down-regulating immune responses.³⁰ Nevertheless, PD-1

expression is primarily induced upon TCR stimulation and lost when T cells fail to receive sustained TCR signaling.³¹ Therefore, we checked whether the MC38-Sia^{null} tumors also contained less antigen-experienced tumor-specific CD8⁺ T cells. Yadav *et al.*²⁹ identified three MC38-specific neoantigens with a strong immunogenic potential. We tested the CD8⁺ T cell reactivity toward these neoantigens by generating tetramers specific for these three identified neoantigens. Isolated CD8⁺ T cells obtained from MC38-MOCK tumors indeed displayed higher reactivity toward two of the neoantigens, while the response to the third antigen showed a trend toward higher recognition (Fig. 4c). The specificity of CD8⁺ T cells in the tumor draining lymph node was indistinguishable between MC38-MOCK and MC38-Sia^{null} groups (Supporting Information Fig. 4B). Together, these results indicate that the MC38-MOCK tumors were infiltrated with more tumor-specific CD8⁺ T cells than MC38-Sia^{null} tumors, thus uncovering a predominant effect of tumor desialylation on the CD8⁺ T cell compartment exclusively in the tumor microenvironment.

MC38-Sia^{null} tumors induce CD8⁺ T cell apoptosis

As the presence of CD8⁺ T cells in the tumor microenvironment correlates with good prognosis,³ we hypothesized that the enhanced growth of the MC38-Sia^{null} tumors was due to hampered elimination by cytotoxic CD8⁺ T cells. Moreover, this appeared to be a local effect, as tumor-specific CD8⁺ T cell frequencies were unaffected in tumor-draining lymph nodes. To explore whether MC38-Sia^{null} cells might be able to suppress the cytotoxic function of CD8⁺ T-cells directly, we performed a cytotoxicity assay using OT-I T cells and OVA-loaded tumor cells as a model system. Activated OT-I CD8⁺ T cells were co-cultured with OVA₂₅₇₋₂₆₄ (SIINFEKL)-pulsed MC38-MOCK and MC38-Sia^{null} cells and assessed for tumor cell eradication. To track the MC38 cells, MC38-MOCK cells were labeled with CFSE and MC38-Sia^{null} with CellVue® Claret (Fig. 5a). After 5 h, OVA₂₅₇₋₂₆₄-pulsed MC38-Sia^{null} cells were less efficiently killed by the OT-I CD8⁺ T cells than the MC38-MOCK cells (Fig. 5b), suggesting that upon encounter of desialylated tumor cells, CD8⁺ T cells are functionally inhibited in their cytotoxic response.

We next investigated whether MC38-Sia^{null} cells are able to influence CD8⁺ T cell function by provoking CD8⁺ T cell death. Interestingly, fewer viable (7-AAD⁻Annexin V⁻) CD8⁺ T cells could be recovered from 48 h co-cultures of wild type C57Bl/6 splenocytes with MC38-Sia^{null} cells, than from splenocytes and MC38-MOCK co-cultures (Fig. 5c). This effect seemed antigen-independent, as it occurred both under medium conditions or when T cells were further stimulated with PHA-L (Fig. 5c). To mimic activated tumor-infiltrating CD8⁺ T cells, we employed antigen-experienced OT-I T cells and investigated whether MC38-Sia^{null} also induced apoptosis of these CD8⁺ T cells without accompanying antigen-specific stimulation. Indeed, at low T cell-tumor ratios, MC38-Sia^{null} cells induced 40% more CD8⁺ T cell apoptosis than MC38-MOCK cells (Fig. 5d).

We next assessed whether the MC38-Sia^{null}-induced apoptosis was mediated by cell-intrinsic factors or *via* the secretion of a soluble factor. Therefore, activated OT-I T cells were co-cultured with MC38-MOCK cells in the presence or absence of supernatants derived from MC38-Sia^{null} cells. Indeed, in the presence of MC38-Sia^{null} supernatant more CD8⁺ T cell apoptosis was measured, indicating that MC38-Sia^{null} cells secrete a soluble pro-apoptotic mediator (Fig. 5e). As the apoptosis induction appeared to be antigen-independent and mediated by a soluble factor in the MC38-Sia^{null} supernatant, we questioned whether MC38-Sia^{null} supernatant alone might be sufficient to cause CD8⁺ T cell apoptosis. To address this, we cultured CD8⁺ T cells only in the presence of supernatants obtained from MC38-MOCK or MC38-Sia^{null} cells or plain medium as a negative control. As expected, CD8⁺ T cell apoptosis was increased by 30% when cells were cultured in the presence of MC38-Sia^{null} supernatant instead of plain medium or MC38-MOCK supernatant (Fig. 5f). To further characterize the apoptosis inducing factor secreted by MC38-Sia^{null} cells, supernatants were heat inactivated prior to addition to the CD8⁺ T cells. Heat inactivation of the MC38-Sia^{null} supernatant completely abrogated CD8⁺ T cell apoptosis (Fig. 5g), suggesting that the MC38-Sia^{null}-specific apoptosis mediator is a heat-sensitive protein or peptide, which acts in an antigen-independent manner.

Moreover, the augmented CD8⁺ T cell apoptosis could provide an explanation for both the reduced CD8⁺ T cell frequencies present in MC38-Sia^{null} tumors as well as the diminished CD8⁺ T cell cytotoxicity toward MC38-Sia^{null} cells *in vitro*.

Low CMAS gene expression is associated with lower recurrence-free survival

So far, our results indicate that loss of sialic acids might actually be detrimental in CRC and thereby contradict other studies investigating the role of tumor sialylation on the anti-tumor immune response.^{15,16,32} To translate our findings to human CRC patients, we analyzed CMAS gene expression in a human colorectal cancer cohort (GSE39582) in relation to disease progression and survival. We stratified the CRC patients according to their CMAS gene expression into two groups, CMAS low (median <150, n = 74) or CMAS high (median >300, n = 81) patients, and evaluated their recurrence-free survival. Interestingly, low CMAS gene expression indeed correlated to a lower recurrence-free survival in CRC patients (Fig. 6a), reflecting the results obtained in our *in vivo* mouse studies. Thus, also in human CRC patients, a low sialylation status of the tumor is correlated to poor prognosis.

Partial tumor desialylation is sufficient to drive tumor growth in CRC

Since low CMAS expression correlated to a lower recurrence-free survival in CRC patients, we tried to mimic this *in vivo* by investigating whether partial tumor desialylation would be enough to sustain the enhanced tumor growth. Therefore, we

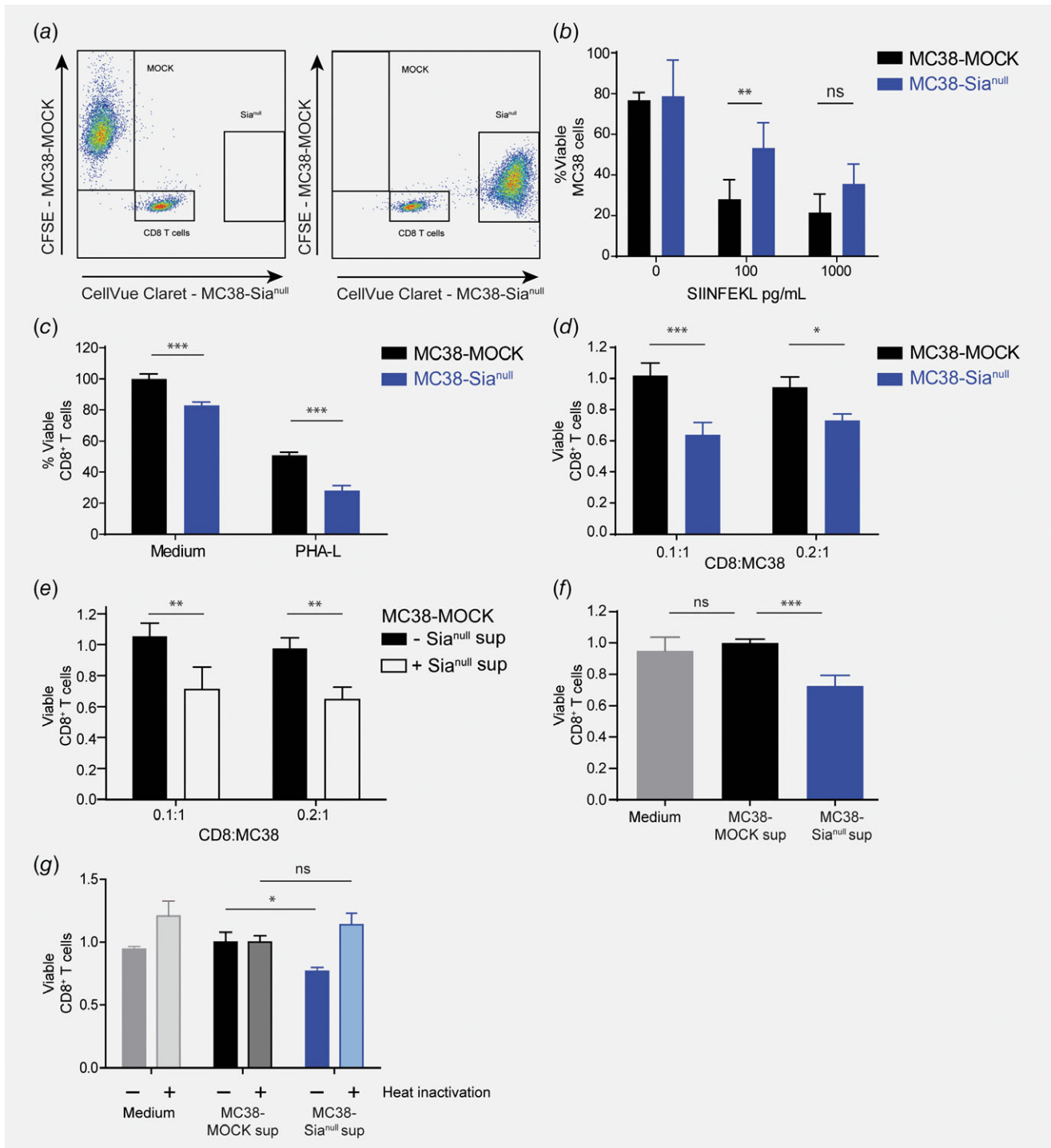


Figure 5. MC38-Sia^{null} cells induce CD8⁺ T cell apoptosis. (a) and (b) MC38-MOCK and MC38-Sia^{null} cells were pulsed with OVA₂₅₇₋₂₆₄ and labeled with CFSE or CellVue Claret respectively (a). After 5 h of incubation with activated OT-I CD8⁺ T cells, viability of MC38 cells was analyzed by flow cytometry and calculated by dividing the number of viable (7-AAD⁻Annexin V⁻) MC38 cells present in the CD8⁺ T cell co-culture by the viable MC38 cells cultured without T cells and multiplied by 100% (b). (c–f) Viable CD8⁺ T cells were analyzed with flow cytometry and gated as CD8b⁺7-AAD⁻Annexin V⁻. (c) C57Bl/6 splenocytes were co-cultured with MC38-MOCK or MC38-Sia^{null} cells in presence of medium or PHA-L for 48 h. (d) Activated OT-I CD8⁺ T cells were co-cultured with MC38-MOCK or MC38-Sia^{null} cells for 24 h. (e) Activated OT-I CD8⁺ T cells were co-cultured with MC38-MOCK in presence of medium or MC38-Sia^{null} supernatant for 24 h. (f) and (g) Activated OT-I CD8⁺ T cells were cultured with control (f) or heat inactivated (g) medium, MC38-MOCK or MC38-Sia^{null} supernatants for 24 h. Data are representative of one (g), two (c, e and f) or three (b and d) independent experiments. Bar, mean ± SD; *, p < 0.05; **, p < 0.01; ***, p < 0.001; ns, not significant. [Color figure can be viewed at wileyonlinelibrary.com]

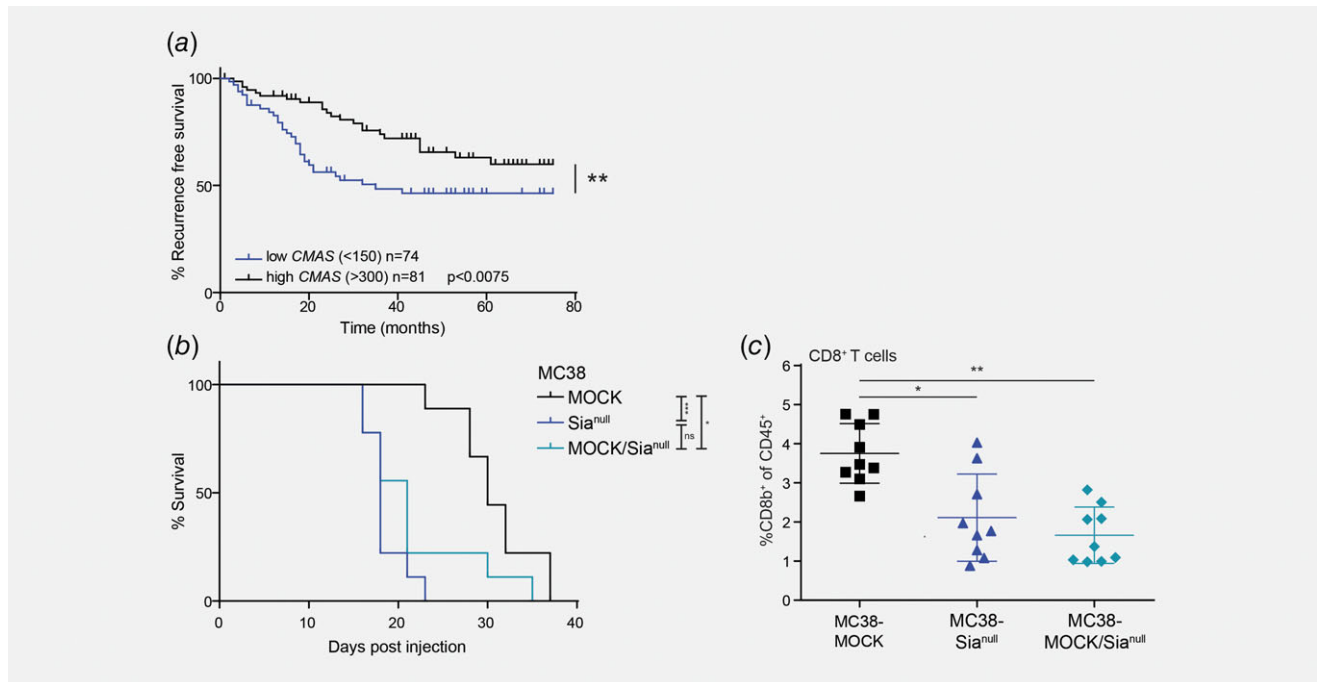


Figure 6. *CMAS* gene expression levels are correlated to recurrence-free survival in human colorectal cancer and a partial *CMAS* knock out is sufficient to drive tumor growth *in vivo*. (a) *CMAS* gene expression data was analyzed in the GSE39582 colorectal cancer cohort.²⁷ Patients were stratified in two groups with either low *CMAS* gene expression (median < 150) or high *CMAS* gene expression (median > 300) and evaluated for their recurrence-free survival. (b) MC38-MOCK, MC38-Sia^{null} or MC38-MOCK cells (30%) mixed with MC38-Sia^{null} cells (70%) were injected into C57Bl/6 mice (n = 9) and sacrificed when the tumor reached a size of 2000 mm³. Tumor growth was measured and survival curves of the mice are displayed. (c) Flow cytometric analysis of viable CD8⁺ T cells (CD3⁺CD8b⁺) at the tumor site when the tumor reached a size of 2000 mm³. Mean ± SD; *, *p* < 0.05; **, *p* < 0.01; ***, *p* < 0.001; ns, not significant. [Color figure can be viewed at wileyonlinelibrary.com]

inoculated mice with MC38-MOCK and MC38-Sia^{null} cells in a 30:70 ratio (MC38-MOCK/Sia^{null}). Interestingly, the survival curve of the mice injected with the mixed tumors followed the survival curve of mice that received MC38-Sia^{null} cells only (Fig. 6b). Moreover, CD8⁺ T cell frequencies were decreased to an equal level as in the MC38-Sia^{null} tumors (Fig. 6c). Together, these data imply that in CRC tumor growth is promoted, even when only a proportion of the malignant cells in the tumor microenvironment is completely desialylated.

Discussion

The upregulation of sialylated glycan structures on the cell surface is a key feature of tumor cells, independent of the tumor type. Sialylated structures are known to regulate immune responses, whereby the current dogma states that tumor cells exploit tumor-associated Sias to dampen anti-tumor immunity.^{14–16} These findings have led to the development of new therapeutic strategies aimed at reducing tumor-associated Sia expression to dismantle the Sia-induced tolerance. However, these novel therapeutic strategies may result in a complete loss of tumor sialylation, yet the effect of a total absence of sialylated structures on tumor growth and anti-tumor immunity has not been investigated before.

Here, we report for the first time that complete abrogation of Sias on the murine CRC cell line MC38 (MC38-Sia^{null}) significantly increased tumor growth *in vivo*. Noteworthy, the MC38 *CMAS* mutated cells were selected in bulk and sorted based on cell surface expression of Sias. In this way tumor heterogeneity was maintained in our cell lines, allowing us to exclude potential clonal effects. Intestinal mucins are known to be both sialylated and/or sulphated,²⁰ yet in the present study we solely affected the sialylation pathway. Therefore, we cannot exclude that sulphated glycans contribute to tumor development in our model.

The increased tumor growth of MC38-Sia^{null} cells could be attributed to reduced CD8⁺ T cell frequencies present within the tumor. Reduced migration of CD8⁺ T cells toward the tumor core has been correlated with bad prognosis.^{2,33,34} As we did not address the localization of the T cells within the tumor microenvironment, we cannot rule out that CD8⁺ T cells were hampered in reaching the tumor core. Nevertheless, we did observe that CD8⁺ T cells displayed diminished cytotoxicity and underwent apoptosis upon encounter of MC38-Sia^{null} cells. Thus, our study highlights that complete tumor desialylation might be detrimental to the anti-tumor immune response in CRC, which greatly complicates the

design of novel cancer therapeutics aimed at targeting the tumor glycosylation profile.

To abrogate cell surface sialylation we knocked out the *CMAS* gene, a catalyzing enzyme involved in the sialylation pathway, whereas other studies focused on the CMP-sialic acid transporter, the *SLC35A1* gene. Although both interrupt the sialylation pathway, the consequences of this interruption might significantly differ, since *SLC35A1* has been described to be involved in the *O*-mannosylation pathway as well.²⁸ E-cadherin, a protein well known for its role in epithelial-to-mesenchymal transition and cancer metastasis,³⁵ is *O*-mannosylated, which is also crucial for E-cadherin-mediated cell adhesion. However, the choice of the target gene cannot fully explain the observed discrepancies. Teoh *et al.*³² recently showed decreased lung metastasis upon *CMAS* gene knock out in a highly metastatic mammary cell line injected in BALB/c mice. We, on the other hand, employed a non-metastatic CRC model that was inoculated in C57BL/6 mice. The different mouse strains, with their different predisposition toward T helper 2 (Th2) and Th1 responses,^{36,37} as well as the different tumor model used, may have impacted the outcome of the respective studies. Discrepancies due to tumor type-specific effects is further supported by the cohort data presented in both studies³² (Fig. 6a). Our CRC cohort analysis revealed that *CMAS* gene expression was positively correlated with prognosis. Strikingly, only a proportion of MC38-Sia^{null} cells was sufficient to sustain the enhanced tumor growth *in vivo*. The analysis of sialoglycans in CRC human tissues and their link to CD8⁺ T cell tumor infiltration are subjects for future studies.

Also in the B16 melanoma model, a reduction in tumor sialylation (B16-Sia^{low}) had a positive effect on the anti-tumor immune response, resulting in decreased tumor growth.^{15,16} Interestingly, the B16 cell line expresses both α 2-3 and α 2-6-linked Sias,¹⁵ while the MC38 cell line only carries α 2-3-linked Sias. This raises the possibility that our findings might be related to the unique presence of α 2-3-linked Sias or conversely the absence of α 2-6-linked Sias. Indeed, humans generally express higher levels of α 2-6-linked Sias than mice.³⁸ Unfortunately, the different functions and roles of α 2-3 and α 2-6-linked Sias and their cognate Siglec receptors in tumor biology are hardly described in literature. In hepatocellular carcinoma, Siglec-1⁺ macrophages negatively associate with progression and predict favorable survival.³⁹ Siglec-1 prefers binding of α 2-3-linked Sias over α 2-6-linked Sias⁴⁰ and lacks the cytoplasmic ITIM domain, common in the majority of Siglec receptors.⁴¹ Intriguingly, Siglec-1⁺ macrophages are able to scavenge Sia⁺-particles from apoptotic tumor cells for subsequent cross-presentation to tumor-specific CD8⁺ T cells.^{42,43} Thus, Siglec-1⁺ macrophages may actually have the potential to propagate anti-tumor immunity.

In light of the lack of α 2-6-linked Sias on our MC38 cells, low and high levels of α 2-6-linked Sias have indeed been correlated to tumor regression or progression, respectively.⁴⁴

Especially, high expression of ST6Gal1, the enzyme responsible for α 2-6-sialylation, has been associated with metastasis and therapeutic failure in colorectal cancer specifically.^{45,46} ST6Gal1 modulates tumor differentiation *in vivo* via an enhanced β 1-integrin function that stimulates cell motility.⁴⁶ These findings suggest that α 2-6-linked Sias may be an important instigator of Sia-mediated immune evasion in CRC. However, conclusive data is lacking to support this hypothesis and should thus be further explored.

One soluble protein known to induce CD8⁺ T cell apoptosis is Galectin-1. Produced by tumor cells, Galectin-1 can bind the Gal β 1-4GlcNAc (LacNAc) epitope,⁴⁷ which is elevated in our MC38-Sia^{null} cells after removal of the Sia. Galectin-1 supports tumor progression through cell–cell and cell-matrix interactions as well as tumor-induced angiogenesis and an elevated CD8⁺ T cell apoptosis.⁴⁸ MC38-Sia^{null} cells indeed showed higher mRNA levels of the *LGALS1* (Galectin-1) gene, however, compared to MC38-MOCK, Galectin-1 protein concentrations in MC38-Sia^{null} supernatants were not increased (data not shown). Therefore, more research is required to identify the soluble factor present in the MC38-Sia^{null} supernatant.

In conclusion, we have demonstrated that complete tumor desialylation of the MC38 mouse CRC cell line augments tumor growth and enhances CD8⁺ T cell apoptosis. Clearly, discrepancies still exist regarding the expression levels or the linkage type of α 2-3 or α 2-6 of Sias and the cellular origins of the tumor. Therefore, the specific impact of α 2-3 and α 2-6-linked Sias and their relative amounts on the anti-tumor immune responses requires further research to fully understand how various tumor types exploit the sialylation machinery to evade anti-tumor immunity. Nevertheless, we argue that in certain tumor types, for instance CRC, tumor sialylation may actually have a protective effect and we suggest that therapies aimed at abrogating tumor-associated Sias should be undertaken with caution.

Acknowledgements

We thank our animal facility for caretaking of the animals and Joke den Haan (Amsterdam UMC) for her advice regarding mouse experiments. We thank Daniel Spencer, Rad Kozak and Max Kotsias (Ludger) for their support regarding the mass spectrometry experiments. We thank the NIH Tetramer Core Facility for providing the MHC–peptide complexes.

Author Contributions

L.A.M.C designed and performed experiments, analyzed data and wrote paper; A.B performed experiments and analyzed data; J.C.H performed experiments; L.K performed subcutaneous cell injections and mouse experiments; A.Z performed mouse experiments; T.O. performed cell sorting experiments; L.W. performed cell culture experiments; Y.v.K and S.v.V conceived and coordinated the study; S.v.V. designed and supervised the study and wrote paper. All authors contributed to reviewing, and/or revising of the study.

References

- Galon J, Costes A, Sanchez-Cabo F, et al. Type, density, and location of immune cells within human colorectal tumors predict clinical outcome. *Science* 2006;313:1960–4.
- Galon J, Pages F, Marincola FM, et al. The immune score as a new possible approach for the classification of cancer. *J Transl Med* 2012;10:1.
- Fridman WH, Pages F, Sautes-Fridman C, et al. The immune contexture in human tumours: impact on clinical outcome. *Nat Rev Cancer* 2012;12:298–306.
- Kim R, Emi M, Tanabe K. Cancer immunoeediting from immune surveillance to immune escape. *Immunology* 2007;121:1–14.
- Varki A, Gagneux P. Biological functions of Glycans. In: rd. In: Varki A, Cummings RD, Esko JD, et al., eds *Essentials of Glycobiology ed.* Cold Spring Harbor, NY, 2015. 77–88.
- Brockhausen I. Mucin-type O-glycans in human colon and breast cancer: glycodynamics and functions. *EMBO Rep* 2006;7:599–604.
- Hakomori S. Cancer-associated glycosphingolipid antigens: their structure, organization, and function. *Acta Anat (Basel)* 1998;161:79–90.
- Pinho SS, Reis CA. Glycosylation in cancer: mechanisms and clinical implications. *Nat Rev Cancer* 2015;15:540–55.
- Crocker PR, Varki A. Siglecs in the immune system. *Immunology* 2001;103:137–45.
- Varki A. Since there are PAMPs and DAMPs, there must be SAMPs? Glycan "self-associated molecular patterns" dampen innate immunity, but pathogens can mimic them. *Glycobiology* 2011;21:1121–4.
- Perdicchio M, Illarregui JM, Verstege MI, et al. Sialic acid-modified antigens impose tolerance via inhibition of T-cell proliferation and de novo induction of regulatory T cells. *Proc Natl Acad Sci USA* 2016;113:3329–34.
- Falco M, Biassoni R, Bottino C, et al. Identification and molecular cloning of p75/AIRM1, a novel member of the sialoadhesin family that functions as an inhibitory receptor in human natural killer cells. *J Exp Med* 1999;190:793–802.
- Nicoll G, Avril T, Lock K, et al. Ganglioside GD3 expression on target cells can modulate NK cell cytotoxicity via siglec-7-dependent and -independent mechanisms. *Eur J Immunol* 2003;33:1642–8.
- Bull C, Boltje TJ, Wassink M, et al. Targeting aberrant sialylation in cancer cells using a fluorinated sialic acid analog impairs adhesion, migration, and in vivo tumor growth. *Mol Cancer Ther* 2013;12:1935–46.
- Perdicchio M, Cornelissen LA, Streng-Ouwehand I, et al. Tumor sialylation impedes T cell mediated anti-tumor responses while promoting tumor associated-regulatory T cells. *Oncotarget* 2016;7:8771–82.
- Bull C, Boltje TJ, Balnegger N, et al. Sialic acid blockade suppresses tumor growth by enhancing T cell-mediated tumor immunity. *Cancer Res* 2018;78:3574–88.
- Stanczak MA, Siddiqui SS, Trefny MP, et al. Self-associated molecular patterns mediate cancer immune evasion by engaging Siglecs on T cells. *J Clin Invest* 2018;128:4912–23.
- Xiao H, Woods EC, Vukojicic P, et al. Precision glycoalkal editing as a strategy for cancer immunotherapy. *Proc Natl Acad Sci U S A* 2016;113:10304–9.
- Ashkani J, Naidoo KJ. Glycosyltransferase gene expression profiles classify cancer types and propose prognostic subtypes. *Sci Rep* 2016;6:26451.
- Robbe C, Capon C, Coddeville B, et al. Structural diversity and specific distribution of O-glycans in normal human mucins along the intestinal tract. *Biochem J* 2004;384:307–16.
- Robbe C, Capon C, Maes E, et al. Evidence of regio-specific glycosylation in human intestinal mucins: presence of an acidic gradient along the intestinal tract. *J Biol Chem* 2003;278:46337–48.
- Robbe-Masselot C, Maes E, Rousset M, et al. Glycosylation of human fetal mucins: a similar repertoire of O-glycans along the intestinal tract. *Glycoconj J* 2009;26:397–413.
- Mihalache A, Delplanque JF, Ringot-Destrez B, et al. Structural characterization of Mucin O-glycosylation may provide important information to help prevent colorectal tumor recurrence. *Front Oncol* 2015;5:217.
- Ran FA, Hsu PD, Wright J, et al. Genome engineering using the CRISPR-Cas9 system. *Nat Protoc* 2013;8:2281–308.
- Kozak RP, Tortosa CB, Fernandes DL, et al. Comparison of procainamide and 2-aminobenzamide labeling for profiling and identification of glycans by liquid chromatography with fluorescence detection coupled to electrospray ionization-mass spectrometry. *Anal Biochem* 2015;486:38–40.
- Ceroni A, Maass K, Geyer H, et al. GlycoWorkbench: a tool for the computer-assisted annotation of mass spectra of glycans. *J Proteome Res* 2008;7:1650–9.
- Marisa L, de Reynies A, Duval A, et al. Gene expression classification of colon cancer into molecular subtypes: characterization, validation, and prognostic value. *PLoS Med* 2013;10:e1001453.
- Riemersma M, Sandrock J, Boltje TJ, et al. Disease mutations in CMP-sialic acid transporter SLC35A1 result in abnormal alpha-dystroglycan O-mannosylation, independent from sialic acid. *Hum Mol Genet* 2015;24:2241–6.
- Yadav M, Jhunjhunwala S, Phung QT, et al. Predicting immunogenic tumour mutations by combining mass spectrometry and exome sequencing. *Nature* 2014;515:572–6.
- Freeman GJ, Long AJ, Iwai Y, et al. Engagement of the PD-1 immunoinhibitory receptor by a novel B7 family member leads to negative regulation of lymphocyte activation. *J Exp Med* 2000;192:1027–34.
- Simon S, Labarriere N. PD-1 expression on tumor-specific T cells: friend or foe for immunotherapy? *Oncoimmunology* 2017;7:e1364828.
- Teoh ST, Ogrodzinski MP, Ross C, et al. Sialic acid metabolism: a key player in breast cancer metastasis revealed by metabolomics. *Front Oncol* 2018;8:174.
- Zhou C, Wu Y, Jiang L, et al. Density and location of CD3(+) and CD8(+) tumor-infiltrating lymphocytes correlate with prognosis of oral squamous cell carcinoma. *J Oral Pathol Med* 2018;47:359–67.
- Melero I, Rouzaut A, Motz GT, et al. T-cell and NK-cell infiltration into solid tumors: a key limiting factor for efficacious cancer immunotherapy. *Cancer Discov* 2014;4:522–6.
- Gheldof A, Bex G. Cadherins and epithelial-to-mesenchymal transition. *Prog Mol Biol Transl Sci* 2013;116:317–36.
- Watanabe H, Numata K, Ito T, et al. Innate immune response in Th1- and Th2-dominant mouse strains. *Shock* 2004;22:460–6.
- Hsieh CS, Macatonia SE, O'Garra A, Murphy KM. T cell genetic background determines default T helper phenotype development in vitro. *J Exp Med* 1995;181:713–21.
- Gagneux P, Cheriyan M, Hurtado-Ziola N, et al. Human-specific regulation of alpha 2-6-linked sialic acids. *J Biol Chem* 2003;278:48245–50.
- Zhang Y, Li JQ, Jiang ZZ, et al. CD169 identifies an anti-tumour macrophage subpopulation in human hepatocellular carcinoma. *J Pathol* 2016;239:231–41.
- Hartnell A, Steel J, Turley H, et al. Characterization of human sialoadhesin, a sialic acid binding receptor expressed by resident and inflammatory macrophage populations. *Blood* 2001;97:288–96.
- Crocker PR, Paulson JC, Varki A. Siglecs and their roles in the immune system. *Nat Rev Immunol* 2007;7:255–66.
- Asano K, Nabeyama A, Miyake Y, et al. CD169-positive macrophages dominate antitumor immunity by crosspresenting dead cell-associated antigens. *Immunity* 2011;34:85–95.
- Goswami KK, Ghosh T, Ghosh S, et al. Tumor promoting role of anti-tumor macrophages in tumor microenvironment. *Cell Immunol* 2017;316:1–10.
- Avidan A, Perlmutter M, Tal S, et al. Differences in the sialylation patterns of membrane stress proteins in chemical carcinogen-induced tumors developed in BALB/c and IL-1alpha deficient mice. *Glycoconj J* 2009;26:1181–95.
- Park JJ, Lee M. Increasing the alpha 2, 6 sialylation of glycoproteins may contribute to metastatic spread and therapeutic resistance in colorectal cancer. *Gut Liver* 2013;7:629–41.
- Hedlund M, Ng E, Varki A, et al. Alpha 2-6-linked sialic acids on N-glycans modulate carcinoma differentiation in vivo. *Cancer Res* 2008;68:388–94.
- Cousin JM, Cloninger MJ. The role of Galectin-1 in cancer progression, and synthetic multivalent Systems for the Study of Galectin-1. *Int J Mol Sci* 2016;17:pii: E1566.
- Stillman BN, Hsu DK, Pang M, et al. Galectin-3 and galectin-1 bind distinct cell surface glycoprotein receptors to induce T cell death. *J Immunol* 2006;176:778–89.